Scientific Research Publishing

Materials Sciences and Applications, 2018, 9, 502-515
http://www.scirp.org/journal/msa
ISSN Online: 2153-1188
ISSN Print: 2153-117X

Mechanical, Thermal and Crystallization Properties of Polypropylene (PP) Reinforced Composites with High Density Polyethylene (HDPE) as Matrix

Harekrushna Sutar[1,2*], Prakash Chandra Sahoo[2], Prateekshya Suman Sahu[2], Surajabala Sahoo[2], Rabiranjan Murmu[2], Sumit Swain[2], Subash Chandra Mishra[1]

[1]Department of Metallurgical and Materials Engineering, National Institute of Technology, Rourkela, India
[2]Department of Chemical Engineering, Indira Gandhi Institute of Technology, Sarang, India
Email: *h.k.sutar@gmail.com

How to cite this paper: Sutar, H., Sahoo, P.C., Sahu, P.S., Sahoo, S., Murmu, R., Swain, S. and Mishra, S.C. (2018) Mechanical, Thermal and Crystallization Properties of Polypropylene (PP) Reinforced Composites with High Density Polyethylene (HDPE) as Matrix. *Materials Sciences and Applications*, **9**, 502-515.
https://doi.org/10.4236/msa.2018.95035

Received: January 11, 2018
Accepted: May 21, 2018
Published: May 24, 2018

Abstract

Our work aims to evaluate a complete outlook of virgin high density polyethylene (HDPE) and polypropylene (PP) polyblends. Virgin PP of 20, 30 and 50 weight% is compounded with virgin HDPE. The properties like tensile strength, flexural strength, Izod impact strength are examined. Scanning electron microscopy (SEM) and polarised light microscopy (PLM) are used to observe the surface and crystal morphology. X-ray diffraction (XRD), Fourier transform infrared spectroscopy (FTIR) tests verify the non compatibility of both polymers. Differential scanning calorimetry (DSC) and thermogravimetric analysis (TGA) techniques are used to study the thermal behaviour of composites. The results manifest co-occurring spherulites for polyblends; indicating the composite to be a physical blend of continuous and dispersed phases, but on the other hand PP improves the tensile and flexural properties of HDPE.

Keywords

High Density Poly Ethylene (HDPE), Polypropylene (PP), Polyblends, Mechanical, Thermal, Crystallization Properties

1. Introduction

Polymer composite is material of research in modern days. Thermoplastic polymers are of great interest due to their technical and commercial importance [1]. In general two or more polymers are melt blended to form a product as polyb-

lends [2] [3] [4] [5]. The component percentages are the primary factor influencing their physical properties [6]. The manufacturing technique and operating conditions are second governing factor.

Among the thermoplastic polymers, PP possesses good mechanical strength. In addition it has high chemical resistance, low cost and easy to manufacture. PP has wide application in automobile spare parts and as well as container [7]. HDPE is known for its large strength to density ratio due to its little branching. HDPE unlike PP cannot withstand normally required autoclaving conditions [8]-[13].

Jia-Horny Lin *et al.* has reinforced HDPE to PP matrix and verified the non-compatibility of both polymers, but improves the impact strength of PP [14]. Souza et al found the effect of processing temperature and content of HDPE on interfacial tension of the PP/HDPE polyblend [15]. Past studies show the compatibility of PP/HDPE polyblends depends on factors like processing temperature, polymer structure and blending ratios [15] [16] [17]. Polymers with similar physical properties form polyblends with greater mechanical strength [18] [19] [20]. The mechanical properties of the PP/HDPE polyblend decreases with increase in dissimilarity of melt flow index (MFI) [21], so we have investigated a complete prospects of PP reinforced HDPE polyblends with similar MFI manufactured by the help of twin screw extruder and injection moulding machines. In addition to mechanical properties; thermal behaviour of the composites are characterised by using DSC, TGA tests. Crystal morphologies are captured using PLM, SEM and X-RD techniques. Compatibility of both the thermoplastics are re-examined by study of molecular structure using FTIR.

2. Experimental

2.1. Collection of Polymers

PP (M110 Grade, homopolymer) produced by the spheripol technology and HDPE (M5818 Grade, injection moulded type) produced by Mitsui Slurry CX technology are purchased from Haldia petrochemical limited, haldia, India. Different physical properties of the polymers are reported in **Table 1**.

2.2. Preparation of Composites

Polymers in the form of pellets are collected. The pellets are dried in a hot air oven at 60˚C for 8 hrs to remove moisture content followed by mixing of 20, 30, and 50 wt% of PP to HDPE. Then they are converted into polymer blend pellets using a twin screw extruder (ZV20, Specific Engineering and Auto Mates, Vadodara, India) at feeder speed of 51 rpm and main rotor at 54 rpm. The screws are of 21 mm diameter and co-rotating type, containing three thermal barrels at 190˚C, 200˚C and 210˚C respectively. The melt and die temperatures are 224˚C and 200˚C.

The obtain pellets are dried at 60˚C for 8 hrs and moulded to test samples using an automatic injection moulding machine (Endura-90, Electonica plastic

Table 1. Physical properties of polymers.

Polymer type	Melt flow index (g/10 min)	Density (g/cc)
HDPE	19 (2.16 kg, 190˚C)	0.956
PP	11 (2.16 kg, 230˚C)	0.900

machines limited, Kolkata, India) with screw diameter of 35 mm at 177 rpm. The temperature of the nozzle is 200˚C and that of the three barrels are 190˚C, 200˚C and 210˚C respectively. Snapshot of the prepared tensile and flexural test samples are shown in **Figure 1**.

2.3. Mechanical Properties

Both tensile and flexural strengths of HDPE/PP polyblends are tested using an universal testing machine (UTM3382, Instron, UK) as per ASTM D638-02a and ASTM D790 standards respectively. Tensile specimens are prepared according to ASTM D638-02a type-I; with gage length 50 mm. Tests are conducted at cross head speed of 50 mm/min. Flexural sample of size 127 mm × 12.7 mm × 3.2 mm are tested at speed of 1.365 mm/min with support span spacing of 51.2 mm (span = 16 times of thickness) at an extension up to 5%. The speed of the test and flexural strengths are calculated according to Equations (1) and (2) respectively.

$$\text{Speed} = \frac{ZL^2}{6d} \tag{1}$$

$$\sigma_{F\max} = \frac{3PL}{2bd^2} \tag{2}$$

where, Z is Rate of straining at 0.01 mm/mm/min, L is span length (mm) and d is sample thickness (mm), $\sigma_{F\max}$ is flexural strength (MPa), P is load (N), L is span length (mm) and b is sample width (mm).

Impact tests are conducted using a Izod and Charpy impactometer (IT 504 Plastic impact , Tinius Olsen ,USA) with a V-notch cutter as per ASTM D256-A standard , possessing a pendulum energy of 13.70 J. Impact test specimens are prepared by cutting the flexural samples to a size of 63.5 mm × 12.7 mm × 3.2 mm with a V-notch of 45˚ and 0.25 mm depth.

2.4. Microscopy Test

Our investigation has used SEM (JEOL; JSM-6480 LV, Japan), Field emission SEM (Nova Nano SEM-450, USA) and PLM (Leica, DM750P, Germany). Morphology of samples is captured before and after fracture of impact test. Energy dispersive spectroscopy (EDS) analysis and carbon mapping test are conducted using FESEM at an operation voltage of 10 KV. Samples are gold coated before each test. PLM is used to observe the spherulite behaviour of the polyblends. A tiny sample is placed on a glass slide and melted at 200˚C (using the hot stage) followed by sandwiching the sample by placing a micro glass slide over it to

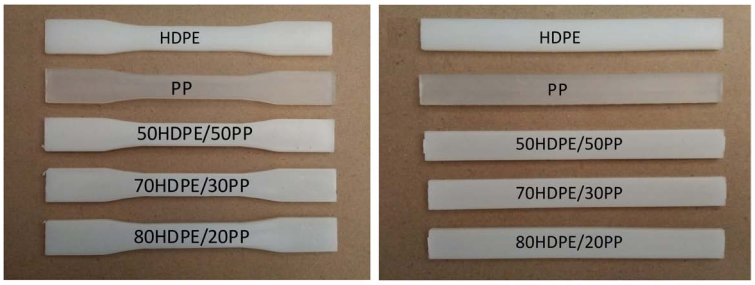

(a) (b)

Figure 1. Snapshot of prepared, (a) tensile and (b) flexural test specimens.

form a thin film. The sample is cooled at 5˚C/min (using cold stage) and spherulite morphologies are captured at 130˚C and 125˚C at magnification × 10.

2.5. XRD and FTIR

In order to analyse any new phase formations after blending the polymers and to understand the chemical structure of the polyblends; the XRD (Philips, PW1720, USA) and FTIR (Perkin-Emler Spectrum 100, USA) techniques are utilised. X-ray scanning is done within a diffraction angle (2θ) range of 10 - 90˚ with Cu Kα radiation at 40 KV and 30 mA. The rate of scanning is 10˚/min and at λ = 0.154 nm. The IR Spectroscopy is observed between the waveband of 450 to 4000 cm^{-1}.

2.6. DSC and TGA Analyses

The polyblends thermal behaviour is analysed using a DSC (Perkin-Elmer DSC 7, MA, USA) and TGA (Perkin-Elmer TGA, MA, USA) analysers. The DSC tests are performed under nitrogen flow rate of 50 ml/min. Polymer samples of around 10 mg are scanned at a heating rate of 10˚C/min from ambient temperature to 200˚C. The samples undergo three thermal cycles. Heating, cooling and reheating under the same condition to follow an identical thermal history for all polymer blends.

The degree of crystallinity (X_C) of the polyblends is evaluated by Equation (3)

$$X_C(\%) = \frac{\Delta H_f}{\text{ø}\Delta H_f^0} \times 100 \tag{3}$$

where, ΔH_f = Melting enthalpy of HDPE or PP in the blend, ΔH_f^0 = Enthalpy corresponding to melting of 100% crystalline HDPE or PP and Ø = weight fraction of HDPE or PP in the blend. In TGA test, polymer samples with masses of approximately 10 mg are heated from atmospheric temperature to 600˚C, at heating rate of 10˚C/min and nitrogen flow rate of 50 ml/min, to observe their degradation behaviour. Data corresponding to ΔH_f^0 are referred from Roger L. Blaine [22].

3. Results and Discussion

3.1. Tensile, Flexural and Impact Strengths

Tensile strength results are shown in **Figure 2(a)**. The maximum value (≈35

MPa) of tensile strength is resulted from PP where as the HDPE matrix bears a tensile strength of ≈22 MPa. Reinforcement of PP to HDPE improves the tensile strength due to formation of brittle polyblends as observable in **Figure 2(b)**. The magnitude of tensile modulus at break point is reported in **Figure 2(c)**. The polyblends of 50 HDPE/50PP shows the maximum (≈146 MPa) value of tensile modulus.

The experimental outcomes for flexural tests are reported in **Figure 3**. Flexural strength improves (See **Figure 3(a)**) and a value of ≈23 MPa is observed for all the composite blends. **Figure 3(b)** reveals the PP added polyblends bear more extension properties when compare to HDPE. Data pertaining to the flexural modulus are reported in **Figure 3(c)**; indicating the PP content increases the flexural modulus; as PP to be a separate phase in the polyblend and HDPE as continuous matrix.

The impact strength of polymers are expressed in three different ways and reported in **Figure 4**. The results corresponding to impact strength in Joule (J) is reported in **Figure 4(a)**; indicating a maximum value for HDPE where as attributing a minimum value to 50/50 polyblend. Energy absorbed during impact per unit thickness of sample is manifested in **Figure 4(b)**. The impact energy absorbed per unit cross sectional area, perpendicular to load; also shows a similar trend as visible in **Figure 4(c)**. Reinforcement of PP particles to HDPE matrices contracts the stress concentration and the plastic deformation property is lost; there by weakening the impact property.

3.2. Phase Analysis

The chemical and crystal structure of HDPE/PP polyblends are analysed by XRD and FTIR. **Figure 5** and **Figure 6** reports the XRD and FTIR results. For PP all the peaks lies between 2θ of 15 to 30˚, which are α form of PP. The peaks are corresponding to crystalline lattices [23]. Two diffraction peaks for HDPE are observed between 20 to 30˚ diffraction angles, comprising of orthorhombic crystals [24] [25]. Reinforcing PP to HDPE does not produce any new peaks, only shortening of peaks for HDPE/PP polyblends are seen. So combination of PP with HDPE is only a physical mixing with no alternation of chemical structure. **Table 2** shows the frequency ranges of different functional groups of PP and HDPE polymers, with assigned vibration type. The FTIR spectra reveals, the peaks of HDPE/PP composites confirms to those of virgin HDPE and PP matrices.

3.3. Thermal Behaviour

From the DSC study the melting temperature (T_m) of PP and HDPE are 168.6 and 134.6˚C respectively. **Table 3** reports the detailed results of melting temperature and melt enthalpy (ΔH_f) of all the polymer type. The HDPE/PP polyblend bears two melt points as shown in **Figure 7(a)**; indicating the polyblend to be a co-occurrence of both HDPE and PP. The results authenticate the polymer

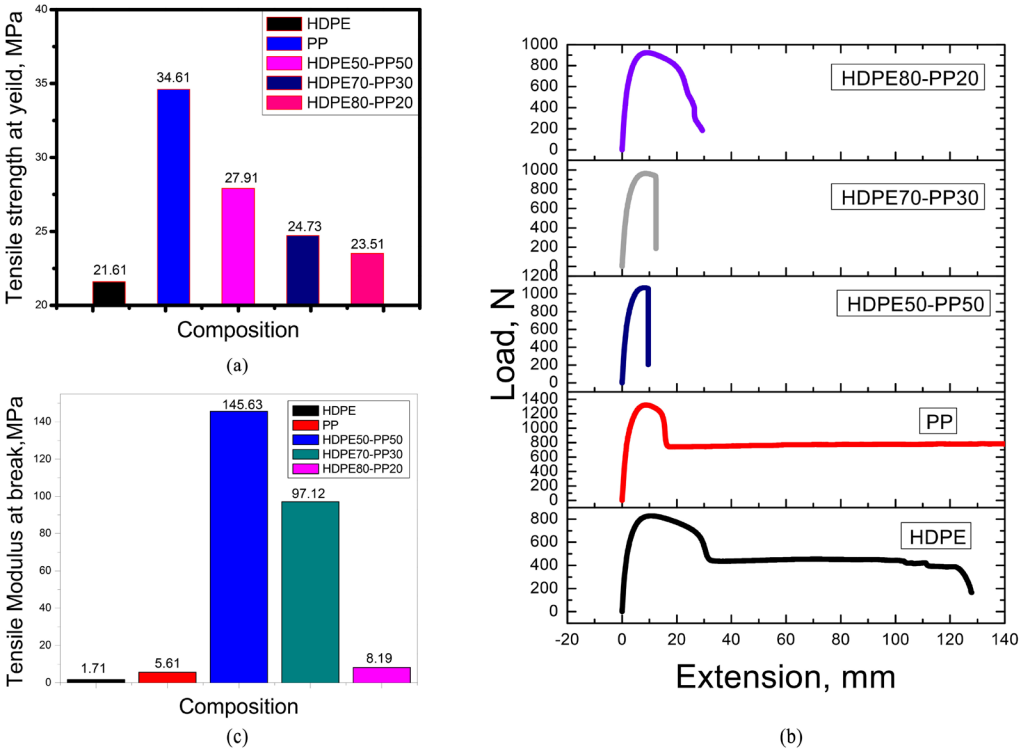

Figure 2. Tensile properties of the polymer composites, (a) tensile strength at yield; (b) load against extension; (c) tensile modulus at break.

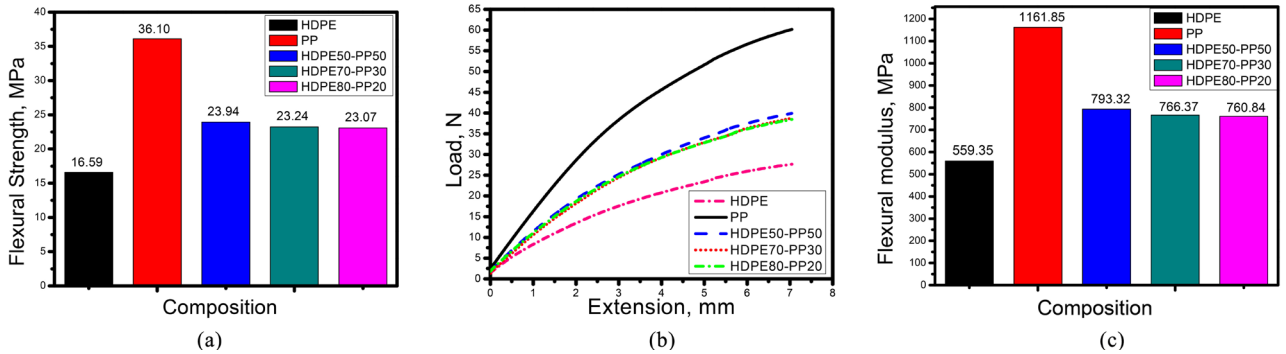

Figure 3. Flexural properties of the polyblends, (a) flexural strength; (b) load vs extension; (c) flexural modulus.

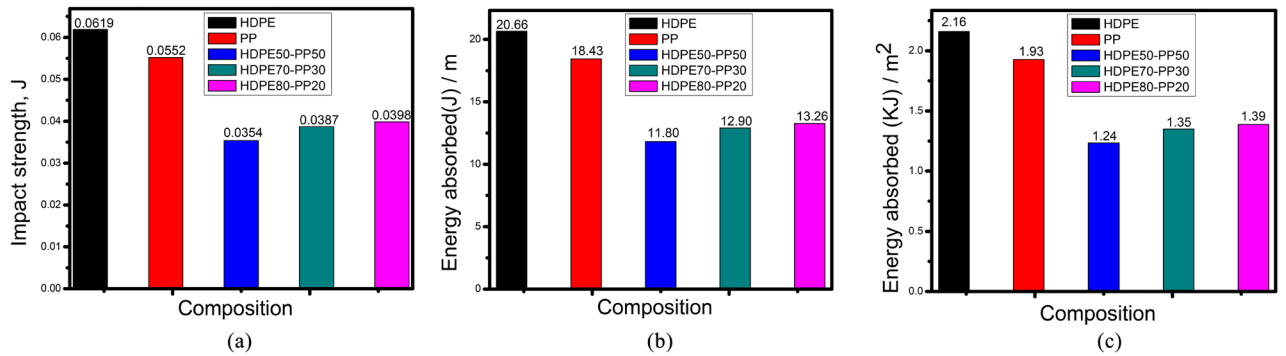

Figure 4. Impact strengths of the polyblends, (a) energy absorbed; (b) energy absorbed/m of sample thickness; (c) energy absorbed/unit cross sectional area.

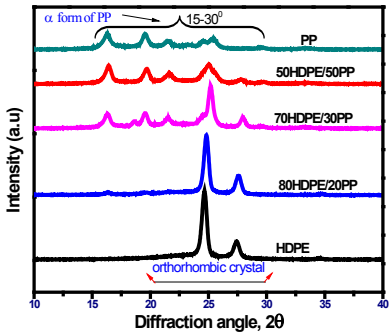

Figure 5. X-Ray diffractogram of polymer composite blends.

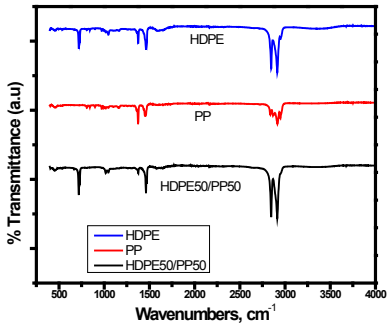

Figure 6. FT-IR spectroscopy of polymer composite blends.

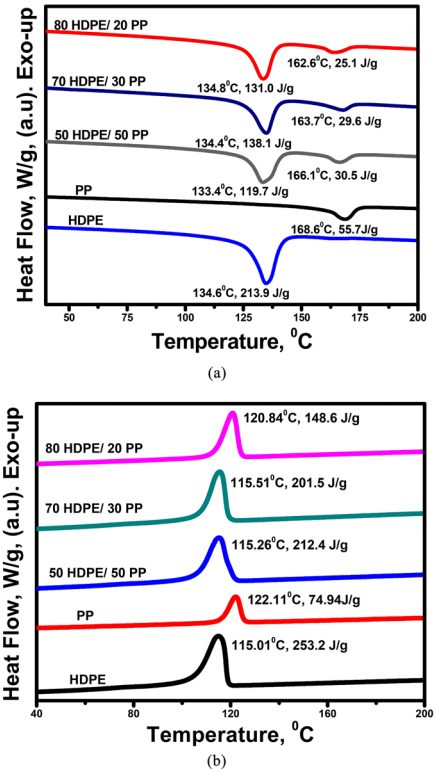

Figure 7. DSC sketches of the obtained polyblends; (a) heating; (b) cooling cycles.

Table 2. IR spectra analysis reports.

Group	Wave number (cm^{-1})	Vibration type	Assigned to
-C-H	2985 - 2810	Stretching	PP
$-CH_2$	2950 - 2850	Stretching	HDPE
$-CH_2$	1475 - 1440	Bending	PP
$-CH_3$	1380 - 1370	Bending	PP
$-CH_2$	1470 - 1460	Bending	HDPE
$-CH_2$	730 - 700	Rocking	HDPE

Table 3. DSC data of HDPE/PP polyblends.

Polymer Type	ΔH_f, J/g	T_m, ˚C	T_c, ˚C	X_c, %	ΔH_c, J/g
HDPE	213.9	134.6	115.0	73.0	253.2
PP	55.7	168.6	122.1	26.9	74.94
50HDPE/50PP	119.7[a]/30.5[b]	134.4[a]/166.1[b]	115.2	81.70[a]/29.46[b]	212.4
70HDPE/30PP	138.1[a]/29.6[b]	134.4[a]/163.7[b]	115.5	67.33[a]/47.66[b]	201.5
80HDPE/20PP	131.0[a]/25.1[b]	134.8[a]/162.6[b]	120.8	55.88[a]/60.62[b]	148.6

The superscript [ab]corresponds to cite HDPE and PP respectively.

composite to be a physical mixture of both the polymers. The existence of PP in HDPE does not alter the melt peak temperature significantly.

Figure 7(b) shows the temperature (T_c) and enthalpy ΔH_c of crystallization for all the polymers resulted from the DSC cooling cycle. The T_c's for PP and HDPE are 122.11˚C and 115.01˚C respectively. Result shows PP crystallizes faster than HDPE. But the order of crystallinity of the composite blend is quite similar to HDPE. Augmentation of PP particles to HDPE retards the nucleation of the heterogeneous polymer blend and so the crystallization peaks of the polyblends are undistinguishable.

The weight loss of a polymer with respect to time or temperature is usually predicted by using TGA technique. The thermal degradation is an irreversible process. Our work focused to predict the degradation temperature (T_D). It is defined in our project as; the temperature at which the weight loss of the polymers just starts to fall immediately. Figure 8 shows TG/DTG thermogram sketches of our prepared polymers. The results obtained via TG analysis on polymers are revealed in Table 4. All the samples undergo a single degradation step. The inflection point (I_p, at which the rate of weight change with temperature is maximum) and residual weight % are also reported in Table 4. It is evident from the results that, the thermal behaviour of the binary polyblends differ marginally; may be due to similar density and MFI.

3.4. Surface Behavior

The surface morphology of polymers before fracture is reported in Figure 9. A

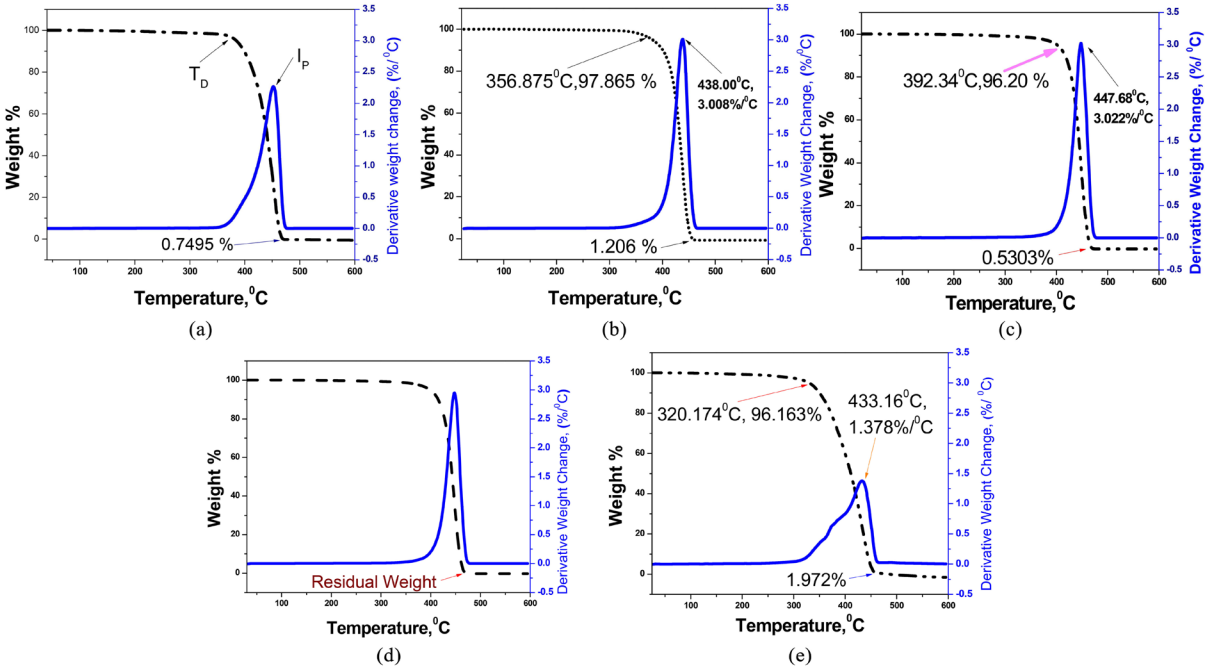

Figure 8. TG/DTG thermograms of (a) virgin HDPE; (b) virgin PP, and HDPE/PP Polyblends which contain; (c) 50 wt%; (d) 30 wt% and (e) 20 wt% of PP.

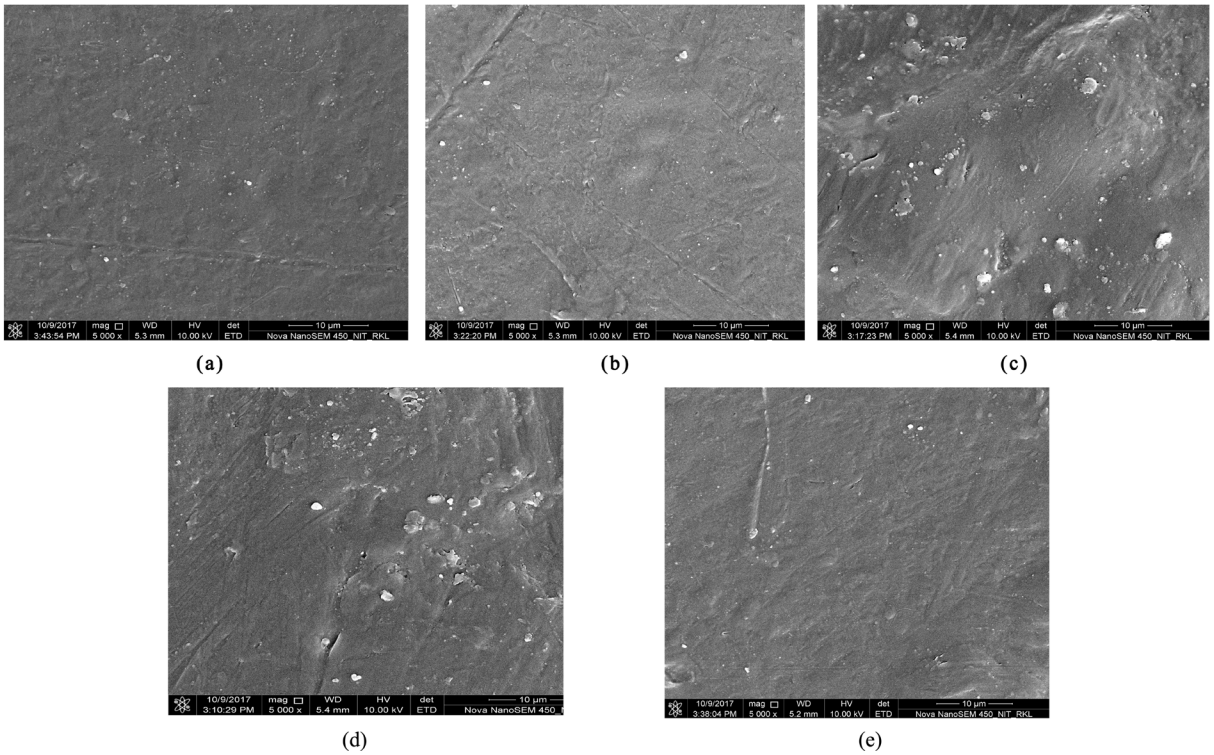

Figure 9. Surface morphology of un-fractured Polyblends; (a) virgin HDPE; (b) virgin PP, and HDPE/PP polyblends which contain; (c) 50 wt%; (d) 30 wt% and (e) 20 wt% of PP.

Table 4. TG/DTG results of prepared polymers.

Sample	T_D, ˚C	Weight % at T_D	Residual weight %	Inflection Point	
				˚C	%/˚C
HDPE	368.56	97.45	0.7495	452.5	2.264
PP	356.87	97.86	1.206	438.0	3.008
50HDPE/50PP	392.34	96.20	0.5303	447.68	3.002
70HDPE/30PP	388.54	96.45	0.6602	447.65	2.94
80HDPE/20PP	320.174	96.16	1.972	433.16	1.378

similar morphology of all the polymer blends is observed. Prepared sample's surfaces are smooth and difficult to differentiate. The continuous and dispersed phases for un-fractured polyblend samples are difficult to identify. To evaluate the changes in the properties; carbon elemental mapping and EDS tests are conducted and disclosed in **Figure 10**. Surface behaviour of fractured specimens after impact test is shown in **Figure 11**. **Figure 11(b)** shows the fractured surface for virgin PP is flat owing to brittle fracture. Fractured virgin HDPE specimen results a wrinkled and aggregative exterior. The ruptured surface of the polyblends is also irregular, owing to their toughness. The reinforcement of PP to HDPE smoothens the surface as visible in **Figures 2(c)-(e)**. The impact energy absorbed falls with augmentation of PP particles (see **Figure 4**), resulting the cracks to prevent bloating due to exerted strain.

Crystal structures of the polyblends during solidification from molten stage are reported in **Figure 12**. Spherulites are large and spherical for PP conforming to the results reported by jia-Horng Lin etal [14], and so called ring spherulites for HDPE. PP forms an overlapped layer in the polyblend and hence an incomplete spherulitic growth is resulting for the polymer composites. Spherulites stalk over each and cannot reach to complete form.

4. Conclusion

Our project promisingly combines PP with HDPE. The dispersion of PP in HDPE improves tensile and flexural strengths. The results show that a 50 wt% PP increases the tensile strength of the composite by 29%, and is maximum among the polymer blends. The magnitude of the flexural strength for all the polyblends are close to 23 MPa and improved by 44%. The XRD, FTIR and DSC tests prove the polyblend to be a combination of two dispersed matrices. No changes in chemical structure are observed, confirming the composite to be a physical blending. PLM tests authenticate; reinforcement of PP particles to HDPE retards the crystal growth and spherulites lap over. TGA tests disclose the degradation characteristics; showing a maximum degradation temperature and weight loss for polymer blends is for composite with 50 wt% PP. Because of the

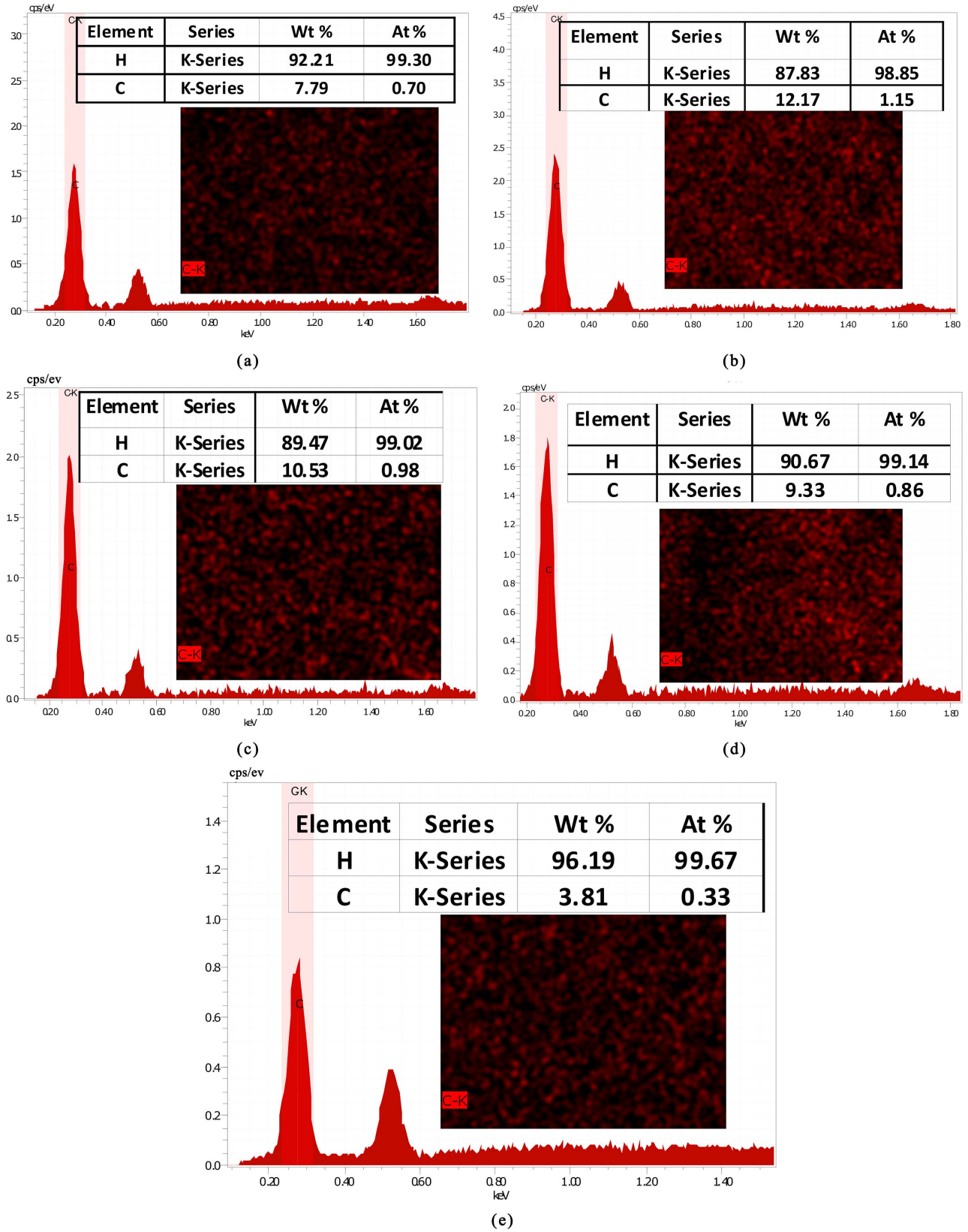

Figure 10. EDS and carbon element mapping of Polyblends; (a) virgin HDPE; (b) virgin PP, and HDPE/PP Polyblends which contain; (c) 50 wt%; (d) 30 wt% and (e) 20 wt% of PP.

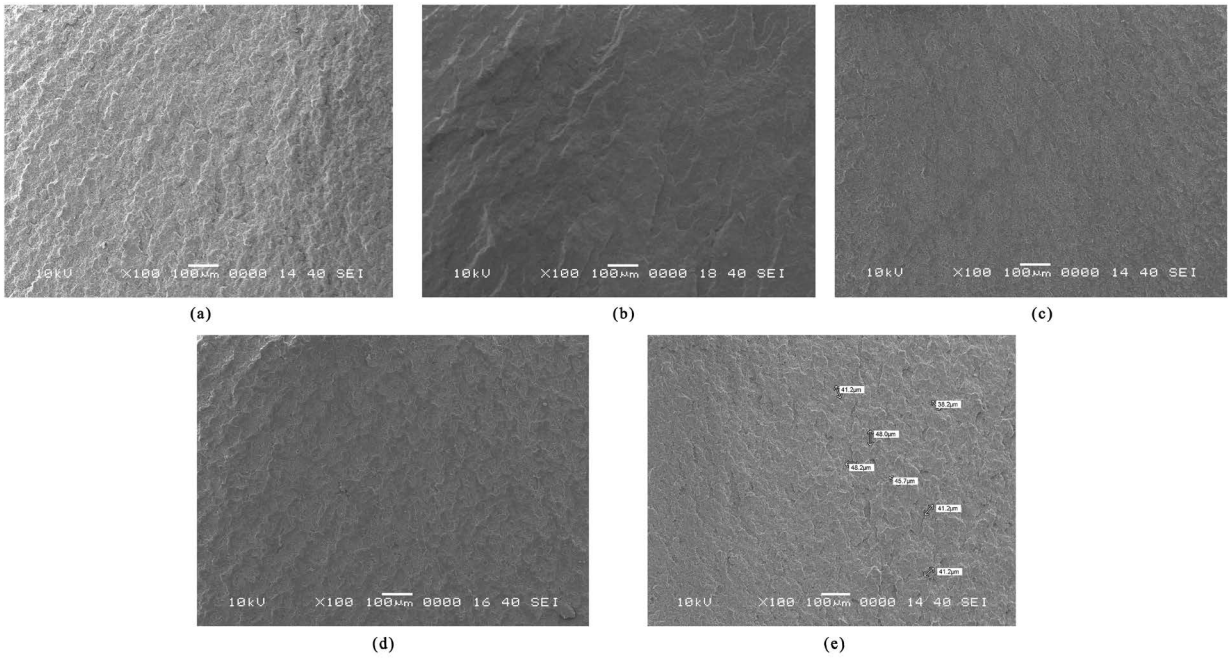

Figure 11. SEM images of the fractured specimens after impact tests; (a) virgin HDPE; (b) virgin PP and polyblends which contain (c) 50 wt %; (d) 30 wt %; (e) 20 wt % of PP.

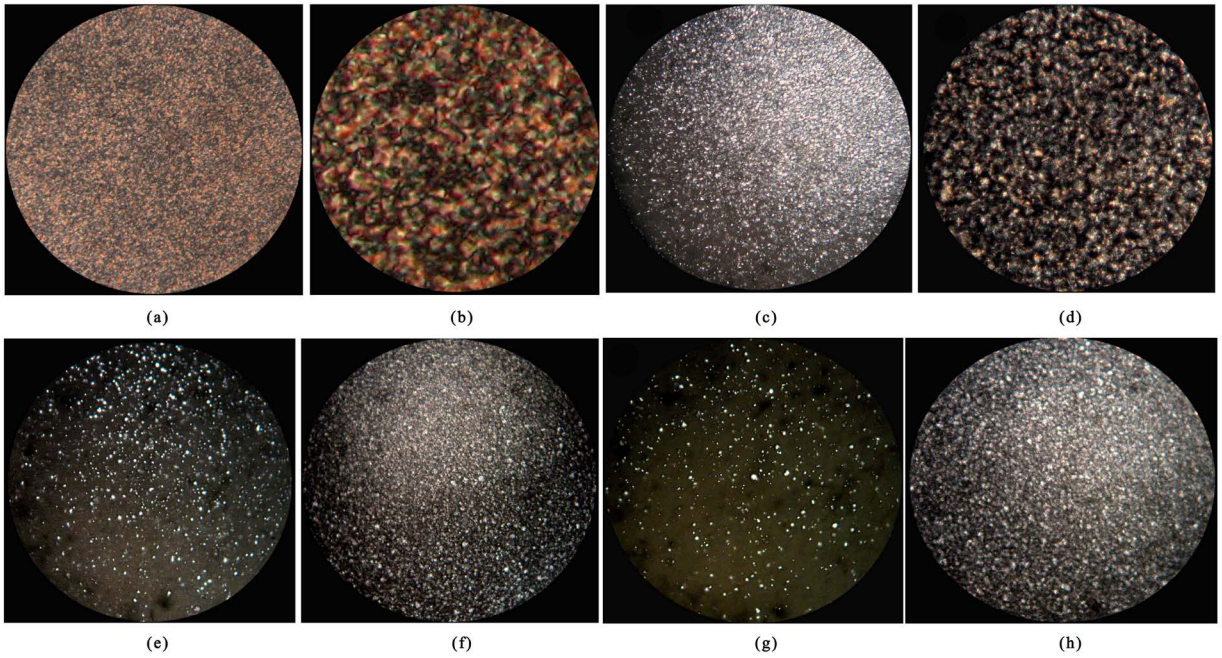

Figure 12. Spherulite structures of prepared polymers (a) HDPE at 130˚C; (b) HDPE at 125˚C; (c) PP at 130˚C; (d) PP at 125˚C; (e) 50HDPE/50PP at 130˚C; (f) 50HDPE/50PP at 125˚C; (g) 80HDPE/20PP at 130˚C; (h) 80HDPE/20PP at 125˚C.

conventional methods are adopted for preparing the HDPE/PP blends with low manufacturing cost, the composite blends may find suitable application areas.

References

[1] Erbetta, C.D.C., Azevedo, R.C.S., Andrade, K.S., e Silva, M.E.S.R. and Roberto,

F.S.F. (2017) Characterization and Lifetime Estimation of High Density Polyethylene Containing a Prodegradant Agent. *Materials Sciences and Applications*, **8**, 979-991. https://doi.org/10.4236/msa.2017.813072

[2] Bertin, S. and Robin, J. (2002) Study and Characterization of Virgin and Recycled LDPE/PP Blends. *European Polymer Journal*, **38**, 2255-2264. https://doi.org/10.1016/S0014-3057(02)00111-8

[3] Laoutid, F., Estrada, E., Michell, R.M., Bonnaud, L., Müller, A.J. and Dubois, P. (2013) The Influence of Nanosilica on the Nucleation, Crystallization and Tensile Properties of PP-PC and PP-PA Blends. *Polymer*, **54**, 3982-3993. https://doi.org/10.1016/j.polymer.2013.05.031

[4] Xie, B.H., Huang, X. and Zhang G.J. (2013) High Thermal Conductive Polyvinyl Alcohol Composites with Hexagonal Boron Nitride Microplatelets as Fillers. *Composites Science and Technology*, **85**, 98-103. https://doi.org/10.1016/j.compscitech.2013.06.010

[5] Ma, W., Zhang, J. and Wang, X. (2008) Crystallizaion and Surface Morphology of Poly(vinylidene fluoride)/Poly(methylmethacrylate) Films by Solution Casting on Different Substrates. *Applied Surface Science*, **254**, 2947-2954. https://doi.org/10.1016/j.apsusc.2007.10.037

[6] Albano, C., González, J., Ichazo, M., Rosales, C., Urbina de Navarro, C. and Parra, C. (2000) Mechanical and Morphological Behavior of Polyolefin Blends in the Presence of CaCO3. *Composite Structures*, **48**, 49-58. https://doi.org/10.1016/S0263-8223(99)00072-0

[7] Hsieh, C.T., Pan, Y.J. and Lin, J.H. (2017) Polypropylene/High-Density Polyethylene/Carbon Fiber Composites: Manufacturing Techniques, Mechanical Properties, and Electromagnetic Interference Shielding Effectiveness. *Fibers and Polymers*, **18**, 155-161. https://doi.org/10.1007/s12221-017-6371-0

[8] Wilkinson, A.N., Laugel, L., Clemens, M.L., Harding, V.M. and Marin, M. (1999) Phase Structure in Polypropylene/PA6/SEBS Blends. *Polymer*, **40**, 4971-4975. https://doi.org/10.1016/S0032-3861(98)00843-X

[9] Tseng, F.P., Lin, J.J. and Tseng, C.R. (2001) Poly (oxypropylene)-Amide Grafted Polypropylene as Novel Compatibilizer for PP and PA6 Blends. *Polymer*, **42**, 713-725. https://doi.org/10.1016/S0032-3861(00)00400-6

[10] Shi, H., Shi, D., Wang, X., Yin, L., Yin, J. and Mai, Y.W. (2010) A Facile Route for Preparing Stable Co-Continuous Morphology of LLDPE/PA6 Blends with Low PA6 Content. *Polymer*, **51**, 4958-4968. https://doi.org/10.1016/j.polymer.2010.08.023

[11] Maciel, A., Salas, V. and Manero, O. (2005) PP/EVA Blends: Mechanical Properties and Morphology. Effect of Compatibilizers on the Impact Behavior. *Advances in Polymer Technology*, **24**, 241-252. https://doi.org/10.1002/adv.20050

[12] Martins, C.G., Larocca, N.M., Paul, D.R. and Pessan, L.A. (2009) Nanocomposites Formed from Polypropylene/EVA Blends. *Polymer*, **50**, 1743-1754. https://doi.org/10.1016/j.polymer.2009.01.059

[13] Valera-Zaragoza, M., Rivas-Vazquez, L.P., Ramirez-Vargas, E., Sánchez-Valdes, S., Ramos-deValle, L.F. and Medellín-Rodríguez, F.J. (2013) Influence of Morphology on the Dynamic Mechanical Characteristics of PP-EP/EVA/Organoclay Nanocomposites. *Composites Part B: Engineering*, **55**, 506-512. https://doi.org/10.1016/j.compositesb.2013.07.009

[14] Lin, J.H., Pan, Y.J., Liu, C.F., Huang, C.L., Hsieh, C.T., Chen, C.K., Lin, Z.Y. and Lou, C.W. (2015) Preparation and Compatibility Evaluation of Polypropylene/High Density Polyethylene Polyblends. *Materials*, **8**, 8850-8859.

https://doi.org/10.3390/ma8125496

[15] Souza, A.M.C. and Demarquette, N.R. (2002) Influence of Composition on the Linear Viscoelastic Behavior and Morphology of PP/HDPE Blends. *Polymer*, **43**, 1313-1321. https://doi.org/10.1016/S0032-3861(01)00718-2

[16] Li, J., Shanks, R.A. and Long, Y. (2000) Mechanical Properties and Morphology of Polyethylene-Polypropylene Blends with Controlled Thermal History. *Journal of Applied Polymer Science*, **76**, 1151-1164. https://doi.org/10.1002/(SICI)1097-4628(20000516)76:7<1151::AID-APP19>3.0.CO;2-H

[17] Jose, S., Aprem, A.S., Francis, B., Chandy, M.C., Werner, P., Alstaedt, V. and Thomas, S. (2004) Phase Morphology, Crystallisation Behaviour and Mechanical Properties of Isotactic Polypropylene/High Density Polyethylene Blends. *European Polymer Journal*, **40**, 2105-2115. https://doi.org/10.1016/j.eurpolymj.2004.02.026

[18] Macosko, C.W., Jeon, H.K. and Hoye, T.R. (2005) Reactions at Polymer-Polymer Interfaces for Blend Compatibilization. *Progress in Polymer Science*, **30**, 939-947. https://doi.org/10.1016/j.progpolymsci.2005.06.003

[19] Saroop, M. and Mathur, G.N. (1997) Studies on the Dynamically Vulcanized Polypropylene (PP)/Butadiene Styrene Block Copolymer (SBS) Blends: Mechanical Properties. *Journal of Applied Polymer Science*, **65**, 2691-2701. https://doi.org/10.1002/(SICI)1097-4628(19970926)65:13<2691::AID-APP10>3.0.CO;2-0

[20] Van Puyvelde, P., Velankar, S. and Moldenaers, P. (2001) Rheology and Morphology of Compatibilized Polymer Blends. *Current Opinion in Colloid and Interface Science*, **6**, 457-463. https://doi.org/10.1016/S1359-0294(01)00113-3

[21] Camacho, W. and Karlsson, S. (2001) NIR, DSC and FTIR as Quantitative Methods for Compositional Analysis of Blends of Polymers Obtained from Recycled Mixed Plastic Waste. *Polymer Engineering and Science*, **41**, 1626-1635. https://doi.org/10.1002/pen.10860

[22] Blaine, R.L. Thermal Applications Note, Polymer Heats of Fusion.

[23] Nishino, T., Matsumoto, T. and Nakamae, K. (2000) Surface Structure of Isotactic Polypropylene by X-Ray Diffraction. *Polymer Engineering and Science*, **40**, 336-343. https://doi.org/10.1002/pen.11167

[24] Inci, B. and Wagener, K.B. (2011) Decreasing the Alkyl Branch Frequency in Precision Polyethylene: Pushing the Limits toward Longer Run Lengths. *Journal of the American Chemical Society*, **133**, 11872-11875. https://doi.org/10.1021/ja2040046

[25] Liao, C.Z. and Tjong S.C. (2012) Mechanical and Thermal Performance of High-Density Polyethylene/Alumina Nanocomposites. *Journal of Macromolecular Science, Part B*, **52**, 812-825. https://doi.org/10.1080/00222348.2012.733297